Progress In Electromagnetics Research M, Vol. 29, 1–15, 2013

EFFECTS OF NONLINEARITY ON WAVE PROPAGATION IN FIBER BRAGG GRATINGS

Aurelia Minut*

Department of Mathematics, Unites States Naval Academy, Annapolis, MD 21402, USA

Abstract—In this paper, we show that the solution of linear coupled mode equations (LCME) is a good approximation to that of the nonlinear coupled mode equations (NLCME) for small times, provided that the nonlinearity is weak. We bound the difference between the two solutions using energy estimates. We illustrate our findings in numerical examples.

1. INTRODUCTION

This work is motivated by the need to examine the behavior of a fiber Bragg grating when large amplitude light is propagated in the fiber. We start with the assumption that the grating has been designed for operation in the linear regime, while the fiber itself has a mild nonlinearity.

A fiber Bragg grating, in its simplest form, is a length of fiber whose index of refraction is periodic in the direction of light propagation. It can be made by exposing a treated fiber to ultraviolet radiation which changes the index of refraction. It has many uses, for instance, filtering and dispersion compensation [6]. It works by coupling the forward- and backward-moving waves in the fiber. The periodicity and the wavelength of light determines the coupling strength.

While it is not the scope of this work to examine the rich phenomena that result from nonlinearity and periodicity, it should be mentioned that some work exploring such aspects as solitons, gap solitons, and light-stopping, exists [3, 4, 9]. In this work, we start with the nonlinear coupled mode equations (NLCME), whose derivation can be found in [9]. It has been pointed out that NLCME is related

Received 3 December 2012, Accepted 28 January 2013, Scheduled 30 January 2013
* Corresponding author: Aurelia Minut (minut@usna.edu).

to light propagation in a fiber modeled by the anharmonic Maxwell-Lorentz equations [5]. Perturbation techniques may be applied to reduce NLCME to the familiar nonlinear Schrödinger's equation, which is more readily analyzed [7, 8]. We mention a related work in [10] where it is shown that nonlinearity in a fiber Bragg grating can lead to pulse splitting in the reflected waves.

The focus of this work is the difference between the solution of the full NLCME and that of its linearized counterpart, the linear coupled mode equations (LCME). Our analysis begins with the energy estimates for NLCME presented in [5]. We show that these energy estimates can be used to bound the difference between the solution of NLCME and that of LCME. We devise a numerical method for integrating NLCME based on the method of characteristics. Numerical calculations are carried out that support our claims.

The contents of this paper are as follows. In Section 2, we give an outline of coupled mode theory leading to the linear and nonlinear coupled mode equations. In Section 3, we introduce our main result, Theorem (3.1), and in Section 4 we present an explicit numerical method for solving NLCME and numerical results illustrating the main findings of this work.

2. COUPLED MODE THEORY

The propagation of light in optical fibers is governed by Maxwell's equations, together with the constitutive relations that describe the interaction of the electromagnetic waves with the medium. In the case of optical fibers, the medium is nonmagnetic and the propagation is restricted to one dimension. Maxwell's equations reduce to [1]

$$\frac{\partial^2 E}{\partial z^2} - \frac{1}{c^2}\frac{\partial^2 E}{\partial t^2} = \mu_0 \frac{\partial^2 P}{\partial t^2}, \tag{1}$$

where μ_0 is the magnetic permeability in vacuum and c the speed of light in vacuum.

In the case of a linear medium, $P(z,t) = \varepsilon_0 \chi^{(1)}(z) E(z,t)$ where ε_0 is the vacuum permittivity. We denote $\varepsilon(z) = 1 + \varepsilon_0 \chi^{(1)}(z)$ and write Equation (1) in the form:

$$\frac{\partial^2 E}{\partial z^2} - \frac{\varepsilon(z)}{c^2}\frac{\partial^2 E}{\partial t^2} = 0.$$

The dielectric constant ε is related to the index of refraction n by $\varepsilon(z) = n^2(z)$. The index of refraction in a fiber Bragg grating is modeled by

$$n(z) = \bar{n} + \Delta n(z) \cos \frac{2\pi z}{\Lambda_0}. \tag{2}$$

Here, $\bar{n}$ denotes the average index of refraction, $\Delta n(z)$ is the modulation depth of the grating and Λ_0 is the reference period of the grating. Light propagating with a frequency ω in a uniform medium with index of refraction $n(z)$ is characterized by a wavenumber $k = \frac{\omega\bar{n}}{c}$.

Coupled mode analysis is based on the idea that if $\Delta n(z)$ is small, the solution to the wave equation can be written as [2]

$$E(z,t) = E_+(z,t)e^{-i(\omega_0 t - k_0 z)} + E_-(z,t)e^{-i(\omega_0 t + k_0 z)} + c.c., \quad (3)$$

where the quantities E_+ and E_- vary slowly with z and t.

The coupling effect is stronger for light with wavelengths at or near the wavelength $\lambda = 2\Lambda_0$, when approximately half a wavelength fits into each period of the grating. This assumption is known as the Bragg condition and is written as

$$\lambda_B = 2\bar{n}\Lambda_0.$$

The wavelength λ_B is called the Bragg wavelength.

Using (3) in (1) with $k_0 = 2\pi/\lambda_B$, we can show that $E_+(z,t)$ and $E_-(z,t)$ satisfy, approximately, the following linear system of coupled mode equations (LCME) [9]:

$$\begin{aligned} i\frac{\partial E_+}{\partial z} + i\frac{\bar{n}}{c}\frac{\partial E_+}{\partial t} + \kappa(z)E_- = 0, \\ -i\frac{\partial E_-}{\partial z} + i\frac{\bar{n}}{c}\frac{\partial E_-}{\partial t} + \kappa(z)E_+ = 0, \end{aligned} \quad (4)$$

where $\kappa(z) = \frac{\pi}{\lambda_B}\Delta n(z)$ represents the local coupling strength.

To model the propagation of light in the nonlinear regime, we assume an instantaneous nonlinear polarization $P_{NL}(z,t) = \chi^{(3)}(z)E^3$. Combining this with Equation (1), we have

$$\frac{\partial^2 E}{\partial z^2} - \frac{\varepsilon(z)}{c^2}\frac{\partial^2 E}{\partial t^2} = \mu_0\frac{\partial^2 P_{NL}}{\partial t^2}.$$

The square of the index of refraction with the addition of nonlinear terms becomes

$$n^2(z,E^2) = \bar{n}^2 + 2\bar{n}\Delta n(z)\cos\frac{2\pi z}{\Lambda_0} + \chi^{(3)}E^2.$$

In this case, the dynamics of the forward and backward propagating waves are described by the nonlinear coupled mode equations (NLCME) [9]:

$$\begin{aligned} i\frac{\partial E_+}{\partial z} + i\frac{\bar{n}}{c}\frac{\partial E_+}{\partial t} + \kappa(z)E_- + \Gamma\left(|E_+|^2 + 2|E_-|^2\right)E_+ = 0, \\ -i\frac{\partial E_-}{\partial z} + i\frac{\bar{n}}{c}\frac{\partial E_-}{\partial t} + \kappa(z)E_+ + \Gamma\left(|E_-|^2 + 2|E_+|^2\right)E_- = 0, \end{aligned} \quad (5)$$

where $\Gamma = \frac{4\pi\varepsilon_0 c\bar{n}n_2}{\lambda_B}$ is the nonlinearity. The quantity n_2 is defined in [1] as $n_2 = \frac{3\chi^{(3)}}{4\varepsilon_0 c\bar{n}^2}$.

3. ENERGY ESTIMATES

In this section, we derive energy estimates for the difference between the solution of (5) and the solution of (4). The L^2 bounds we obtain show that for relatively small times, the solution of NLCME can be controlled by the solution of LCME.

For a proof of the following propositions, we refer to [5]. Note that in [5], the notation T is used for the "slow time variable" εt.

Proposition 3.1 *If* $\mathbf{E} = (E_+, E_-)$ *is a solution of (5), then the* L^2 *norm of* $\mathbf{E}$ *is preserved; i.e., the energy* $||\mathbf{E}||_2^2 = \int(|E_+|^2 + |E_-|^2)dz$ *is conserved.*

Proposition 3.2 *Let* $\mathbf{E} = (E_+, E_-)$ *satisfy the system (5) with initial conditions* $\mathbf{E}(0) \in H^s$ *for* $s \geq 1$. *Then there exists* $C_s = C_s(||\mathbf{E}(0)||_{H^s}, T)$ *such that* $||\mathbf{E}(T)||_{H^s} \leq C_s(||\mathbf{E}(0)||_{H^s}, T)$.

Theorem 3.1 *Let* (E_+, E_-) *be a solution of the NLCME (5) and let* (E_+^0, E_-^0) *be a solution of the LCME (4). Let* $e_+ = E_+ - E_+^0$ *and* $e_- = E_- - E_-^0$ *and let* $||\mathbf{e}||_{L^2}^2 = \int_{\mathbb{R}}(|e_+|^2 + |e_-|^2)dz$. *Then*

$$||\mathbf{e}(t)||_{L^2}^2 \leq C_1 e^{C_2 t} + C_3 e^{C_4 t},$$

where C_i, $i = 1, 2, 3, 4$ *are constants and depend on* Γ, t *and* $||\mathbf{e}(0)||_{L^2}$.

Proof. The NLCME system (5) can be written as:

$$\begin{aligned} &\frac{\partial E_+}{\partial z} + v\frac{\partial E_+}{\partial t} - i\kappa(z)E_- - i\Gamma(|E_+|^2 + 2|E_-|^2)E_+ = 0, \\ &\frac{\partial E_-}{\partial z} - v\frac{\partial E_-}{\partial t} + i\kappa(z)E_+ + i\Gamma(|E_-|^2 + 2|E_+|^2)E_- = 0, \end{aligned} \tag{6}$$

where $v = \frac{\bar{n}}{c}$ and the LCME system (4) as:

$$\begin{aligned} &\frac{\partial E_+^0}{\partial z} + v\frac{\partial E_+^0}{\partial t} - i\kappa(z)E_-^0 = 0, \\ &\frac{\partial E_-^0}{\partial z} - v\frac{\partial E_-^0}{\partial t} + i\kappa(z)E_+^0 = 0. \end{aligned}$$

With e_+ and e_- defined above, they satisfy:

$$\begin{aligned} &\frac{\partial e_+}{\partial z} + v\frac{\partial e_+}{\partial t} - i\kappa(z)e_- - i\Gamma\left(|E_+|^2 + 2|E_-|^2\right)E_+ = 0, \\ &\frac{\partial e_-}{\partial z} - v\frac{\partial e_-}{\partial t} + i\kappa(z)e_+ + i\Gamma\left(|E_-|^2 + 2|E_+|^2\right)E_- = 0. \end{aligned} \tag{7}$$

We start by taking the first of (7) and multiplying it by $\overline{e_+}$. Next we take the complex conjugate of the first of (7) and multiply it by e_+.

The resulting equations are added to obtain:

$$\frac{\partial}{\partial z}|e_+|^2+\nu\frac{\partial}{\partial t}|e_+|^2+i\kappa(z)\left(\overline{e_-}e_+-\overline{e_+}e_-\right)$$
$$+i\Gamma(|E_+|^2+2|E_-|^2)\left(\overline{E_+}e_+-\overline{e_+}E_+\right)=0.$$

A similar operation is done to the second of (7), and the resulting equation is subtracted from the above result to get:

$$\begin{aligned}&\frac{\partial}{\partial t}\left(|e_+|^2+|e_-|^2\right)\\ =\;&-\frac{1}{v}\frac{\partial}{\partial z}|e_+|^2+\frac{1}{v}\frac{\partial}{\partial z}|e_-|^2+\frac{i\Gamma}{v}\left(\left(|E_+|^2+2|E_-|^2\right)\left(E_+\overline{e_+}-\overline{E_+}e_+\right)\right.\\ &\left.+\left(|E_-|^2+2|E_+|^2\right)\left(E_-\overline{e_-}-\overline{E_-}e_-\right)\right).\end{aligned}$$

Next, we evaluate the last term of the above inequality

$$\begin{aligned}&\left|\left(|E_+|^2+2|E_-|^2\right)\left(E_+\overline{e_+}-\overline{E_+}e_+\right)+\left(|E_-|^2+2|E_+|^2\right)\left(E_-\overline{e_-}-\overline{E_-}e_-\right)\right|\\ \le&2|E_+||e_+|\left(|E_+|^2+2|E_-|^2\right)+2|E_-||e_-|\left(|E_-|^2+2|E_+|^2\right)\\ \le&\left(\left(|E_+|^2+2|E_-|^2\right)|E_+|\right)^2+|e_+|^2+\left(\left(|E_-|^2+2|E_+|^2\right)|E_-|\right)^2+|e_-|^2\\ \le&|e_+|^2+|e_-|^2+\frac{7}{2}\left(|E_+|^2+|E_-|^2\right)^3\end{aligned}$$

Hence

$$\begin{aligned}&\frac{\partial}{\partial t}\left(|e_+|^2+|e_-|^2\right)\\ \le&-\frac{1}{v}\frac{\partial}{\partial z}|e_+|^2+\frac{1}{v}\frac{\partial}{\partial z}|e_-|^2+\frac{\Gamma}{v}\left(|e_-|^2+|e_+|^2+\frac{7}{2}\left(|E_+|^2+|E_-|^2\right)^3\right)\end{aligned}\quad(8)$$

Integrating (8) on $\mathbb{R}$, we get

$$\frac{d}{dt}\|\mathbf{e}\|_{L^2}^2\le\Gamma\|\mathbf{e}\|_{L^2}^2+\frac{7\Gamma}{2v}\int_R\left(|E_+|^2+|E_-|^2\right)^3\,dz.\quad(9)$$

Let

$$\|\mathbf{E}\|_{L^2}^2=\int_{\mathbb{R}}\left(|E_+|^2+|E_-|^2\right)dz,\quad(10)$$

and

$$\|\mathbf{E}\|_{L^\infty}=\max(|E_+|_{L^\infty},|E_-|_{L^\infty}).$$

With this notation, the last term of (9) becomes

$$\begin{aligned}\int_{\mathbb{R}}\left(|E_+|^2+|E_-|^2\right)^3dz\le&\int_{\mathbb{R}}\left(|E_+|+|E_-|\right)^4\left(|E_+|^2+|E_-|^2\right)dz\\ \le&\int_{\mathbb{R}}\left(2\sup(|E_+|,|E_-|)\right)^4\left(|E_+|^2+|E_-|^2\right)dz\\ \le&16\int_{\mathbb{R}}\|\mathbf{E}\|_{L^\infty}^4\left(|E_+|^2+|E_-|^2\right)dz.\end{aligned}$$

From Proposition 3.2, for small time t and a constant C_1, we have that

$$\|\mathbf{E}(t)\|_{L^\infty} \leq \|\mathbf{E}(0)\|_{L^\infty} e^{C_1 t/2}.$$

Therefore, putting this in the inequality above, we get

$$\int_{\mathbb{R}} (|E_+|^2 + |E_-|^2)^3 \, dz \leq 16 e^{2C_1 t} \|\mathbf{E}(0)||_{L^\infty}^4 \|\mathbf{E}(t)\|_{L^2}^2.$$

Therefore (9) becomes

$$\frac{d}{dt}\|\mathbf{e}\|_{L^2}^2 \leq \Gamma \|\mathbf{e}\|_{L^2}^2 + \frac{56\Gamma}{v} e^{2C_1 t} ||\mathbf{E}(0)||_{L^\infty}^4 ||\mathbf{E}(t)||_{L^2}^2.$$

Using Gronwall's inequality we get

$$\|\mathbf{e}\|_{L^2}^2 \leq \|\mathbf{e}(0)\|_{L^2}^2 e^{\Gamma t} + \frac{56\Gamma}{v} ||\mathbf{E}(0)||_{L^\infty}^4 \int_0^t e^{\Gamma(t-s)} e^{2C_1 s} ||\mathbf{E}(s)||_{L^2}^2 ds \quad (11)$$

Again, from Proposition 3.2 (C_2 is a constant and time t is small), we have

$$\|\mathbf{E}(t)\|_{L^2} \leq \|\mathbf{E}(0)\|_{L^2} e^{C_2 t/2}$$

and Equation (11) becomes

$$\|\mathbf{e}\|_{L^2}^2 \leq \|\mathbf{e}(0)\|_{L^2}^2 e^{\Gamma t} + \frac{56\Gamma ||\mathbf{E}(0)||_{L^\infty}^4 ||\mathbf{E}(0)||_{L^2}^2}{v(-\Gamma + 2C_1 + C_2)} \left(e^{(2C_1 + C_2)t} - e^{\Gamma t} \right).$$

This completes the proof of Theorem 3.1.

4. NUMERICAL COMPUTATION

In this section we present numerical results for the nonlinear coupled mode equations (NLCME) for fiber Bragg gratings. We solve numerically NLCME (5) as an initial value problem. We assume that the fiber has length $2L$ and that the left half is filled with homogeneous nonlinear material while the right half has the grating. The initial conditions for the forward (right) going wave, E_+ is zero for $z > 0$ and a Gaussian centered at $-L/2$ for $z < 0$. The backward (left) going wave, E_- is zero at t=0.

Given $\kappa(z)$ and Γ in (5), we want to solve for $E_+(z, t)$ and $E_-(z, t)$. By introducing the normalized time variable, $t' := \frac{c}{\bar{n}} t$ we can simplify the system (5). Dropping the prime on the new time variable, we get

$$\begin{aligned} i\frac{\partial E_+}{\partial z} + i\frac{\partial E_+}{\partial t} + \kappa(z) E_- + \Gamma \left(|E_+|^2 + 2|E_-|^2 \right) E_+ = 0, \\ -i\frac{\partial E_-}{\partial z} + i\frac{\partial E_-}{\partial t} + \kappa(z) E_+ + \Gamma \left(|E_-|^2 + 2|E_+|^2 \right) E_- = 0. \end{aligned} \quad (12)$$

4.1. A Numerical Method

A method of characteristics is chosen to solve the above system. We introduce the following characteristic variables: $\xi = (t - z)/2$ and $\eta = (t + z)/2$. Then the system (12) becomes

$$\begin{aligned} i\frac{\partial E_+}{\partial \eta} + \kappa(z)E_- + \Gamma\left(|E_+|^2 + 2|E_-|^2\right)E_+ = 0, \\ i\frac{\partial E_-}{\partial \xi} + \kappa(z)E_+ + \Gamma\left(|E_-|^2 + 2|E_+|^2\right)E_- = 0. \end{aligned} \tag{13}$$

Consider the points $A(z_0, t_0)$, $B(z_0 + 2h, t_0)$, and $C(z_0 + h, t_0 + h)$. It can be seen that A and C are on the line $\xi = (t_0 - z_0)/2$, and B, C are on the line $\eta = (t_0 + z_0)/2 + h$, as indicated in Figure 1.

Given the fields at time $t = 0$, we integrate along the characteristics to get the fields at time $t = h$, after the space z is sampled at intervals of length $2h$. See Figure 2. Integrating the first equation of (13) along the line AC ($\xi = \text{const.}$), and the second equation along the line BC ($\eta = \text{const.}$), we get

$$\begin{aligned} i(E_+(C) - E_+(A)) + \int_A^C \left(\kappa(z)E_- + \Gamma\left(|E_+|^2 + 2|E_-|^2\right)E_+\right)d\eta = 0, \\ i(E_-(C) - E_-(B)) + \int_B^C \left(\kappa(z)E_+ + \Gamma\left(|E_-|^2 + 2|E_+|^2\right)E_-\right)d\xi = 0. \end{aligned} \tag{14}$$

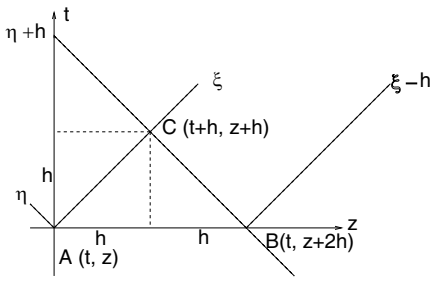

Figure 1. Characteristic coordinates.

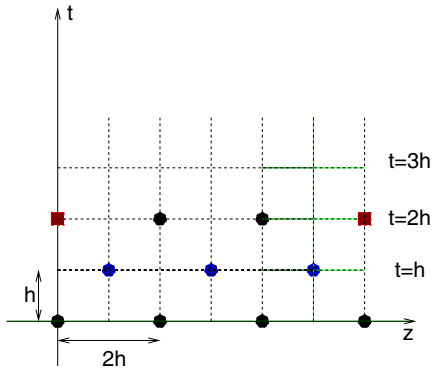

Figure 2. Discretization.

Using the trapezoidal rule to compute the integrals, we get

$$\begin{aligned}
&i(E_+(C)-E_+(A))+\frac{h}{2}(\kappa(C)E_-(C)+\kappa(A)E_-(A))+\frac{h\Gamma}{2}\left(|E_+(C)|^2\right.\\
&\left.+2|E_-(C)|^2\right)E_+(C)+\frac{h\Gamma}{2}\left(|E_+(A)|^2+2|E_-(A)|^2\right)E_+(A)=0,\\
&i(E_-(C)-E_-(B))+\frac{h}{2}(\kappa(C)E_+(C)+\kappa(B)E_+(B))+\frac{h\Gamma}{2}\left(|E_-(C)|^2\right.\\
&\left.+2|E_+(C)|^2\right)E_-(C)+\frac{h\Gamma}{2}\left(|E_-(B)|^2+2|E_+(B)|^2\right)E_-(B)=0.
\end{aligned} \tag{15}$$

Separating the terms at C from the terms at A and B and denoting

$$F_A = iE_+(A) - \frac{h}{2}\kappa(A)E_-(A) - \frac{h}{2}\Gamma\left(|E_+(A)|^2 + 2|E_-(A)|^2\right)E_+(A)$$

and

$$F_B = iE_-(B) - \frac{h}{2}\kappa(B)E_+(B) - \frac{h}{2}\Gamma\left(|E_-(B)|^2 + 2|E_+(B)|^2\right)E_-(B)$$

we get

$$\left[\begin{pmatrix} i & \frac{h}{2}\kappa(C) \\ \frac{h}{2}\kappa(C) & i \end{pmatrix}+\frac{h}{2}\Gamma\begin{pmatrix} |E_+(C)|^2+2|E_-(C)|^2 & 0 \\ 0 & |E_-(C)|^2+2|E_+(C)|^2 \end{pmatrix}\right]$$
$$\begin{pmatrix} E_+(C) \\ E_-(C) \end{pmatrix} = \begin{pmatrix} F_A \\ F_B \end{pmatrix}.$$

If we denote

$$M = \begin{pmatrix} i & \frac{h}{2}\kappa(C) \\ \frac{h}{2}\kappa(C) & i \end{pmatrix},$$

the above equation becomes

$$M\cdot\begin{pmatrix} E_+(C) \\ E_-(C) \end{pmatrix}+\frac{h\Gamma}{2}\begin{pmatrix} \left(|E_+(C)|^2+2|E_-(C)|^2\right)E_+(C) \\ \left(|E_-(C)|^2+2|E_+(C)|^2\right)E_-(C) \end{pmatrix}=\begin{pmatrix} F_A \\ F_B \end{pmatrix}. \tag{16}$$

If we assume that $h\Gamma \ll 1$, we can write

$$\begin{pmatrix} E_+(C) \\ E_-(C) \end{pmatrix}=\begin{pmatrix} E_+^{(0)}(C) \\ E_-^{(0)}(C) \end{pmatrix}+(h\Gamma)\begin{pmatrix} E_+^{(1)}(C) \\ E_-^{(1)}(C) \end{pmatrix}+(h\Gamma)^2\begin{pmatrix} E_+^{(2)}(C) \\ E_-^{(2)}(C) \end{pmatrix}+\ldots. \tag{17}$$

With the expansion given above,

$$|E_\pm(X)|^2 = \left|E_\pm^{(0)}(X)\right|^2 + 2(h\Gamma)\mathrm{Re}\left(E_\pm^{(0)}(X)\bar{E}_\pm^{(1)}(X)\right) \tag{18}$$

where $X = A, B, C$. Let

$$E(C) = \begin{pmatrix} E_+(C) \\ E_-(C) \end{pmatrix},$$

then using (17), $E(C)$ can be written as

$$E(C) = E^{(0)}(C) + (h\Gamma)E^{(1)}(C) + (h\Gamma)^2 E^{(2)} + \dots. \tag{19}$$

Using (16), (17), (18) and (19) we get

$$M\cdot E^{(0)}(C)+(h\Gamma)M\cdot E^{(1)}(C)+\frac{h\Gamma}{2}\begin{pmatrix}\left(|E_+^{(0)}(C)|^2+2|E_-^{(0)}(C)|^2\right)E_+^{(0)}(C)\\ \left(|E_-^{(0)}(C)|^2+2|E_+^{(0)}(C)|^2\right)E_-^{(0)}(C)\end{pmatrix}$$

$$=\begin{pmatrix}F_A\\F_B\end{pmatrix}.$$

Then

$$E^{(0)}(C) = M^{-1}\begin{pmatrix}F_A\\F_B\end{pmatrix}.$$

and

$$E^{(1)}(C) = -\frac{1}{2}M^{-1}\begin{pmatrix}(|E_+^{(0)}(C)|^2 + 2|E_-^{(0)}(C)|^2)E_+^{(0)}(C)\\ (|E_-^{(0)}(C)|^2 + 2|E_+^{(0)}(C)|^2)E_-^{(0)}(C)\end{pmatrix}.$$

The truncation error due to the numerical integration scheme is of order $O(h^3)$. As $h \to 0$, the truncation error $|L_h(\xi,\eta)| \to 0$, thus the method is consistent. However, the discrete scheme is not expected to conserve energy due to the quadrature error and the approximation of the solution. It is possible to derive a Crank-Nicolson scheme which conserves energy. However, such a scheme does not have as good dispersion properties as the characteristic scheme and is also implicit.

4.2. Examples

We choose the initial condition $E_+ = 3.25 * e^{-200(\frac{z+\frac{L}{2}}{L})^2}$, $E_- = 0$, the mesh size $h = \frac{2L}{N-1}$, where N is the number of points in the discretization. The following parameters were used in the calculations.

L	10^{-4} [m]
$\bar{n}$	1.46
$\Delta n(z)$	$0.01e^{-500(\frac{z-L/2}{L})^6}$
Λ_0	0.53545×10^{-6} [m]
λ_B	1.55×10^{-6} [m]
Γ	2.5×10^{-16} [m/V^2]

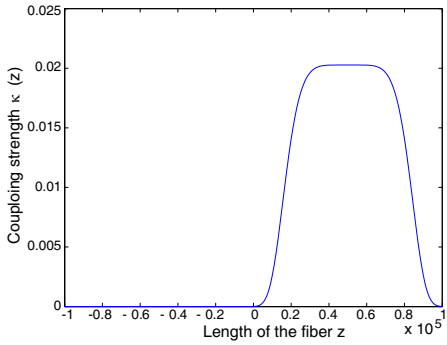

Figure 3. Coupling strength $\kappa(z)$.

The profile of the coupling coefficient $\kappa(z)$ is shown in Figure 3.

We show the evolution of the system for $\Gamma = 2.5 \times 10^{-16}\,[\mathrm{m/V^2}]$. The initial data are shown in Figure 4(a). The fields $E_+(z,\,t)$ and $E_-(z,\,t)$ are shown at times $t = 0.2,\, 0.4,\, 0.8 \times 10^{-3}$ ns in Figures 4(b)–(d). The most noticeable effect is that the nonlinearity changes the shape and the phase in the propagating pulse.

A graph of the energy defined in (10) is shown in Figure 5. The numerical scheme does not conserve energy due to quadrature error and approximate solution to the nonlinear equation. However, for small nonlinearities the deviation in energy is small. As we can see in Figure 5, the energy deviates most from its correct value only when the waves interact with the inhomogeneities in the material; i.e., where $\kappa'(z) \neq 0$. The maximum deviation for $\Gamma = 2.5 \times 10^{-16}\,[\mathrm{m/V^2}]$ is about 1.5%.

To assess the effect of nonlinearity, we computed the reflected pulse at time $t = 0.8 \times 10^{-3}$ ns for various values of Γ. The results are shown in Figure 6 where we display the real and imaginary parts of $E_-(z,t)$. The values of Γ are 0, 2×10^{-16}, 4×10^{-16}, and $10 \times 10^{-16}\,[\mathrm{m/V^2}]$.

Next we calculated the reflected pulse amplitude for various nonlinearities at location $z = -0.5 \times 10^5$ nm. The result of these calculations are shown in Figure 7. This point is chosen because it is the point where the amplitude of the initial condition for the right-going wave reaches its peak, as it is shown in Figure 8. If there is no nonlinearity, then the reflected pulse at this location will simply be a copy of the incident pulse except that it is imaginary (90° phase). It can be seen that the amplitude is not very sensitive to the level of nonlinearity. The phase, however, is more sensitive to the nonlinearity. We calculated the phase at the peak amplitude of the reflected pulse.

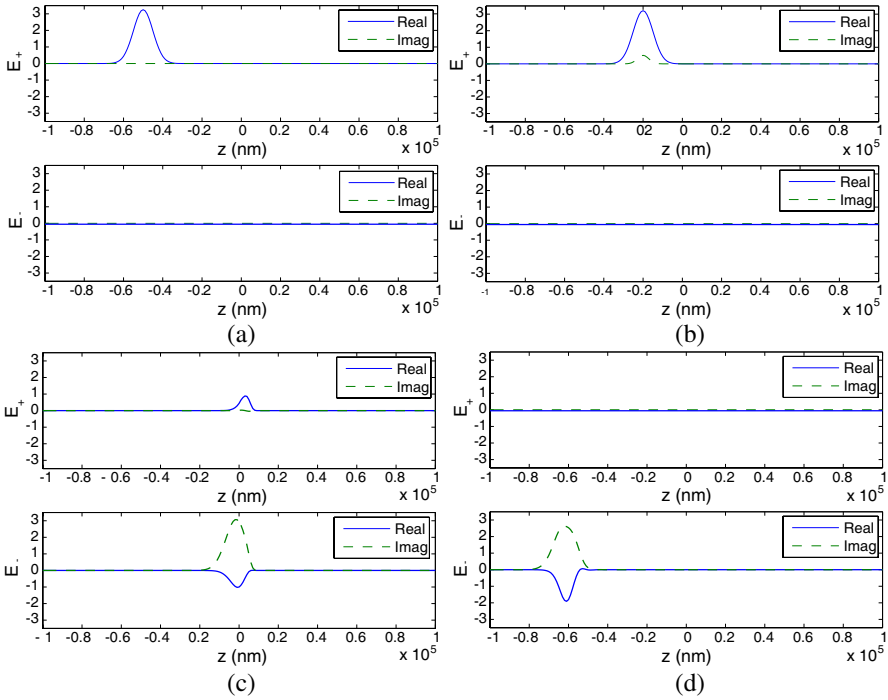

Figure 4. Reflection of a pulse by a fiber Bragg grating. Shown in (a) is the initial data. (b)–(d) are the snapshots of the fields E_+ (top) and E_- (bottom) at times 2, 4, 8×10^{-4} ns.

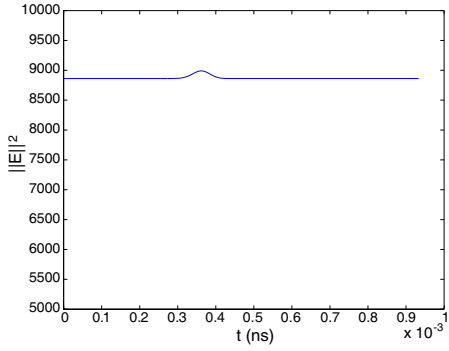

Figure 5. Energy (10) as a function of time. Note that deviation from conservation is very small (about 1.5%) and occurs only when the waves interact with the medium inhomogeneity.

As a reference, the phase is 90° for linear fiber Bragg grating. The results of this calculation are shown in Figure 9 where it can be seen that the phase depends almost linearly on Γ in the regime of weak nonlinearity.

Finally, to assess the effect of nonlinearity versus the required

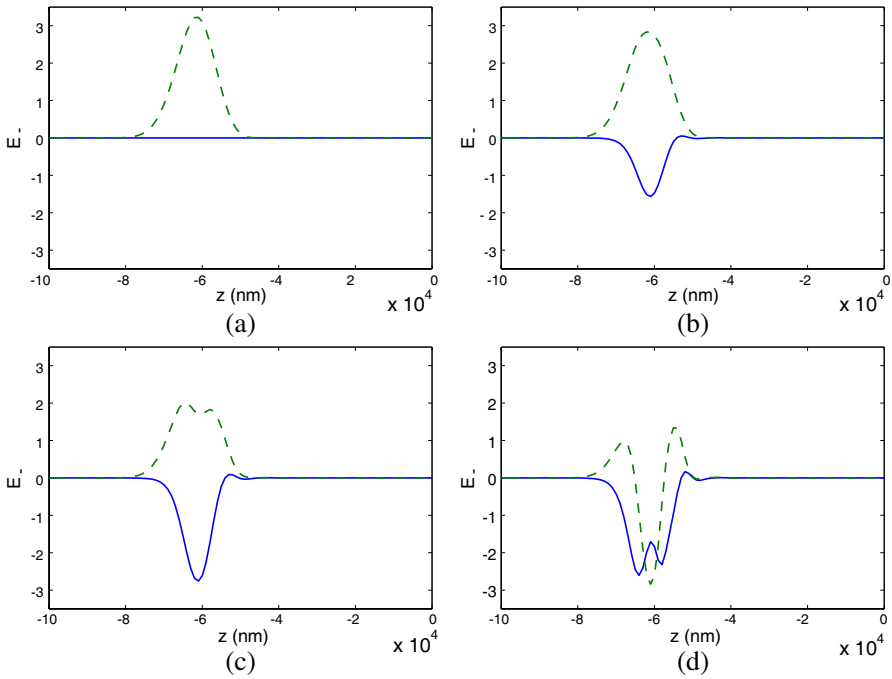

Figure 6. Reflected left-going field for different levels of nonlinearity. The real (solid line) and imaginary (dashed line) parts of $E_-(z, t)$ are shown. The values of Γ are, from (a) to (d), 0, 2×10^{-16}, 4×10^{-16}, and 10×10^{-16} [m/V^2]. Horizontal axis is in units of 10^4 nm.

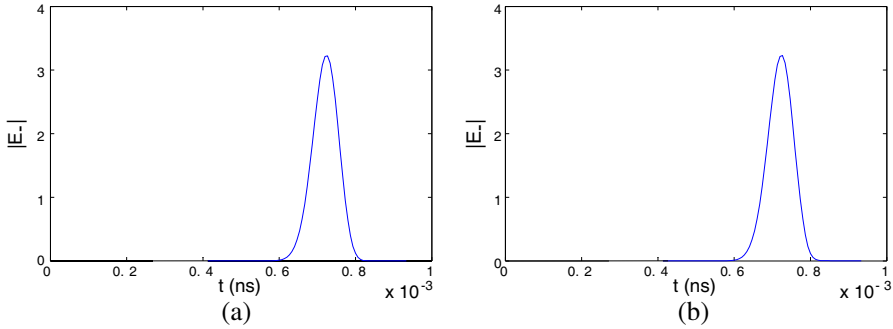

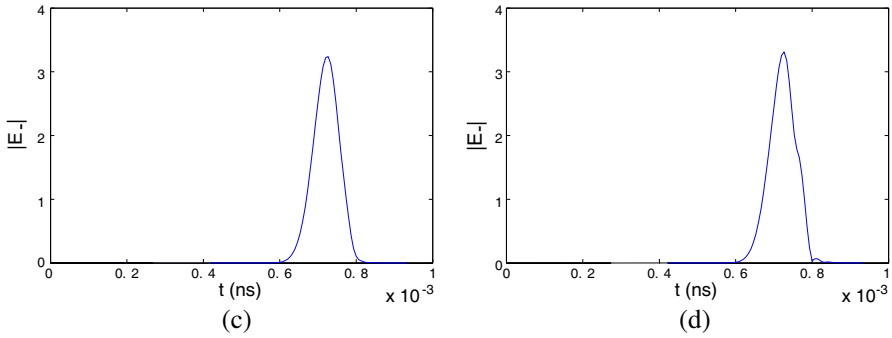

Figure 7. The reflected pulse amplitude at location $z = -0.5 \times 10^5$. The values of Γ are, from (a) to (d), 0, 2×10^{-16}, 4×10^{-16}, and 10×10^{-16} [m/V^2]. Horizontal time axis is in units of 10^{-3} ns.

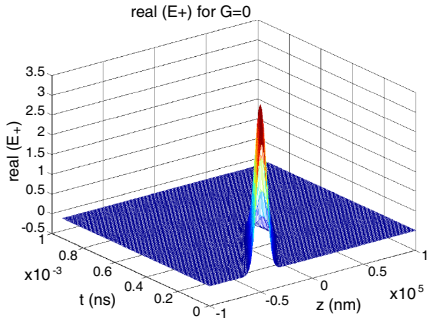

Figure 8. The real part of the transmitted pulse. The maximum amplitude is located at $z = -0.5 \times 10^5$.

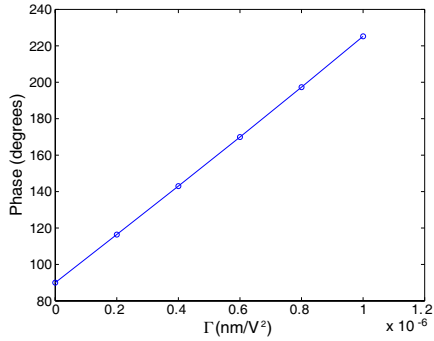

Figure 9. The phase of the reflected pulse at its peak amplitude at $z = -0.5 \times 10^5$ as a function of nonlinearity. The incident pulse has phase equal to zero at its peak at the same point.

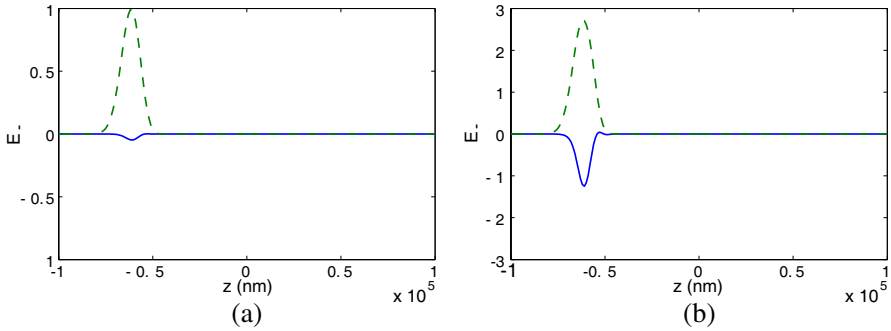

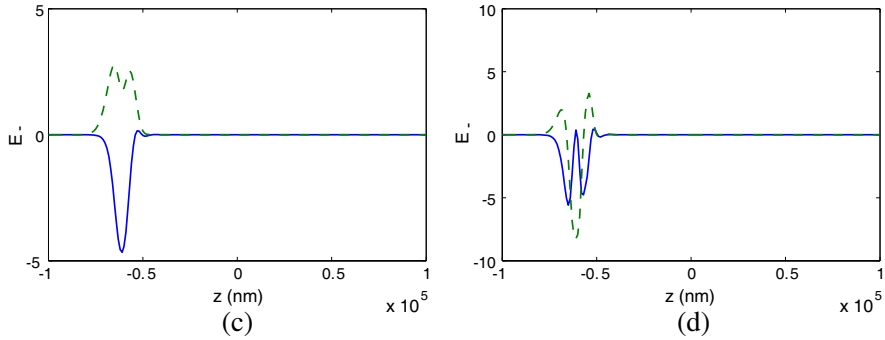

Figure 10. Reflected left-going field for different initial amplitudes for E_+. The real (solid line) and imaginary (dashed line) parts of $E_-(z,\, t)$ are shown. The values of $|E_+|$ are, from (a) to (d), 1, 3, 5, and 8. Horizontal time axis is in units of 10^5 nm and the nonlinearity is $\Gamma = 2.5 \times 10^{-16}\,[\mathrm{m/V^2}]$. Note that for higher power levels, the nonlinear effect is quite apparent.

electric field to produce certain distortion, we computed the reflected pulse at time $t = 0.8 \times 10^{-3}$ ns for various initial values of $|E_+|$. The results are shown in Figure 10 where we display the real and imaginary parts of E_-. The values of $|E_+|$ are, from (a) to (d), 1, 3, 5, and 8.

5. DISCUSSION

We have investigated the effect of nonlinearity on wave propagation in a fiber Bragg grating. The method for analysis, and for solving the nonlinear coupled mode equations, can be extended to the case where the fiber has an index offset and chirp. Our result shows that the solution of the nonlinear coupled mode equation remains close to that of the linear coupled mode equation for small nonlinearities and small travel distances. These findings were further substantiated in numerical simulations. The result presented here gives further evidence that weak nonlinearities present little or no impairment to the performance of a fiber Bragg grating.

ACKNOWLEDGMENT

The author thanks Fadil Santosa of Department of Mathematics, University of Minnesota, for many helpful discussions.

REFERENCES

1. Agrawal, G. P., *Nonlinear Fiber Optics*, 3rd Edition, Academic Press, 2006.
2. Eggleton, B. J., C. M. de Sterke, and R. E. Slusher, "Nonlinear pulse propagation in Bragg gratings," *J. Opt. Soc. Am. B*, Vol. 14, 2980–2993, 1997.
3. Eggleton, B. J., C. M. de Sterke, and R. E. Slusher, "Bragg solitons in the nonlinear Schrodinger limit: Experiment and theory," *J. Opt. Soc. Am. B*, 587–599, 1999.
4. Eggleton, B. J., R. E. Slusher, C. M. de Sterke, P. A. Krug, and J. E. Sipe, "Bragg grating solitons," *Phys. Rev. Lett.*, Vol. 76, 1627–1630, 1996.
5. Goodman, R. H., M. I. Weinstein, and P. J. Holmes, "Nonlinear propagation of light in one-dimensional periodic structures," *J. Nonlin. Sci.*, Vol. 11, 123–168, 2001.
6. Kashyap, R., *Fiber Bragg Gratings*, Academic Press, 1999.
7. Slusher, R. E., B. J. Eggleton, T. A. Strasser, and C. M. de Sterke, "Nonlinear pulse reflections from chirped fiber gratings," *Opt. Express*, Vol. 3, 465–475, 1998.
8. De Sterke, C. M., "Wave propagation through nonuniform gratings with slowly varying parameters," *J. Lightwave Technol.*, Vol. 17, 2405–2411, 1999.
9. De Sterke, C. M. and J. E. Sipe, "Gap solitons," *Progress in Optics XXXIII*, Chap. III, 203–260, 1994.
10. Tsoy, E. N. and C. M. de Sterke, "Propagation of nonlinear pulses in chirped gratings," *Phys. Rev. E*, Vol. 62, No. 2, 2882–2890, 2000.